Evolution of magnetic anisotropy and spin-reorientation transition in Fe films grown on GaAs(113)*A* substrates by molecular-beam epitaxy

P. K. Muduli,[a] J. Herfort, H.-P. Schönherr, and K. H. Ploog
Paul-Drude-Institut für Festkörperelektronik, Hausvogteiplatz 5-7, Berlin 10117, Germany

(Received 17 May 2004; accepted 18 April 2005; published online 20 June 2005)

The magnetic properties of Fe films grown on GaAs(113)*A* substrates by molecular-beam epitaxy are studied using superconducting quantum interference device magnetometry for a wide range of thickness varying from 3.5 monolayers (MLs) to 100 nm (714 MLs). The first signature of ferromagnetism is found at a nominal coverage of about 4 MLs, attributed to a percolation phenomenon, similar to Fe on GaAs(001). The magnetic anisotropy of all samples is found to be a combination of varying strengths of an in-plane uniaxial magnetic anisotropy (UMA) and a four-fold magnetic anisotropy. Samples of thickness $d_{\mathrm{Fe}} \leqslant 50$ MLs exhibit a dominating UMA with the easy and hard axes along $[33\bar{2}]$ and $[\bar{1}10]$, respectively, whereas samples of thickness $d_{\mathrm{Fe}} \geqslant 70$ MLs exhibit a dominating four-fold magnetic anisotropy with the easy axes along the in-plane $\langle 03\bar{1} \rangle$ directions. The reorientation of the easy axis from $[33\bar{2}]$ to the in-plane $\langle 03\bar{1} \rangle$ axes is found to take place between 50 and 70 MLs, the same thickness range where the relaxation of the layer starts. The effective uniaxial magnetic anisotropy constant K_u^{eff} first increases with monolayer coverage up to about 10 MLs and then decreases with the increase in thickness. On the other hand, the effective four-fold anisotropy constant K_1^{eff} first increases with monolayer coverage and then saturates close to the bulk value after about 20 MLs. From a comparison of our results with literature a common origin of UMA in Fe films on GaAs(001) and (113)*A*, i.e., the anisotropy of the bonding of Fe with As and Ga at the interface is anticipated. © *2005 American Institute of Physics*. [DOI: 10.1063/1.1929852]

I. INTRODUCTION

Ferromagnetic metals on semiconductor substrates offer a possibility to realize spin-based devices, i.e., devices that use both the spin and the charge of the electron.[1–3] Fe, having a lattice mismatch of only −1.4% with GaAs and having a high Curie temperature of 1040 K (for bulk Fe), is a promising candidate for such applications. Because of the small lattice mismatch, the stable bcc phase of Fe grows epitaxially on GaAs(001), GaAs(110), GaAs(113)*A*, and GaAs(133)*A* substrates, and numerous studies optimizing its growth conditions and analyzing its interface structure have been reported.[4–13] For efficient spin injection to be achieved, intermixing of Fe with Ga and/or As has to be minimized, which is believed to be detrimental to spin-dependent transmission across the interface.[12] For this reason most of the previous studies of Fe growth were performed on Ga-terminated GaAs(001) templates, at a growth temperature close to room temperature (RT), to avoid interface reactions between Fe and GaAs.[11–13] However, we have recently demonstrated that Fe growth on As-terminated GaAs surfaces is superior to that on Ga-terminated surfaces in removing macroscopic defects on the surface.[13] Moreover, spin injection of Fe into GaAs was achieved due to this optimized growth conditions.[14]

Single-crystal Fe films on GaAs also offer an opportunity of studying magnetism at low dimension with controllable magnetic properties. It is well known that ultrathin Fe films on GaAs(001) substrates below a certain thickness exhibit a dominant in-plane uniaxial magnetic anisotropy (UMA) with the easy and hard axes along [110] and $[\bar{1}10]$, respectively,[7,11,15–17] which is unexpected from the crystal symmetry of Fe. The origin of this UMA can not be understood from the combination of common anisotropy energies, such as magnetocrystalline anisotropy, demagnetizing field energy and magnetoelastic coupling energy. Krebs *et al.* added a uniaxial anisotropy term to the total magnetic anisotropy energy to understand the observed magnetic properties in this system.[18] More recently, Thomas *et al.*[19] pointed out that for a quantitative modeling of the thickness dependence of the magnetic anisotropy, a strain anisotropy mediated by a magnetoelastic coupling term has to be included though they ruled out magnetoelastic coupling as a cause for the observed UMA. To get further insight into the magnetic properties of the Fe/GaAs system, we have chosen the [113]*A* orientation of GaAs for three different reasons. First, the reconstructed surface of GaAs(113)*A* exhibits a step structure,[20–22] which is expected to modify the magnetic properties. Second, such a system could be useful to understand the origin of UMA in the Fe/GaAs system. Third, it is shown in literature that the GaAs(113)*A* substrate, being a high-index substrate, acts as an excellent template for growing semiconductor nanostructures.[23–28] Thus, it might be suitable for growing magnetic nanostructures of Fe, where the magnetic properties can be manipulated. In addition, for the (113) surface of Fe, none

[a]Electronic mail: muduli@pdi-berlin.de

of the bulk easy axes (the ⟨001⟩ directions) lies in plane, thus making it an interesting system for the study of shape anisotropy.

This paper is organized in the following way. In Sec. II experimental details of the preparation of the GaAs template, the growth of Fe, and its basic structural characterizations are discussed. Section III presents the results obtained with *ex situ* superconducting quantum interference device (SQUID) magnetometry in three subsections dealing with the onset of ferromagnetism, UMA in ultrathin films, and in-plane fourfold anisotropy of thick films in the Fe/GaAs(113)*A* system. In Sec. IV we discuss an analytical model to explain the observed magnetic properties. The phenomena involving the onset of ferromagnetism and the possible origin of uniaxial magnetic anisotropy in the Fe/GaAs system, in general, are also discussed.

II. EXPERIMENT

Fe films in the thickness range of 3.5 monolayers (MLs) to 100 nm (714 MLs) were epitaxially grown on GaAs(113)*A* substrates by molecular-beam epitaxy (MBE). The GaAs(113)*A* templates were prepared in a separate III-V growth chamber under As-rich conditions. The growth temperature for the GaAs buffer layer was 610 °C. All Fe samples presented in this article were grown on an (8×1) reconstructed GaAs(113)*A* surface, obtained by cooling the substrate after the buffer layer growth under As_4 flux to 400 °C.[13] The (8×1) reconstruction of GaAs was found to be very stable down to 0 °C. Fe films were grown in an As-free metal chamber connected to the III-V growth chamber through an ultrahigh vacuum interlock. The growth temperature of Fe was maintained at 0 °C with a typical growth rate of 1.2 ML/min, where we assume a thickness of 0.14 nm for 1-ML coverage similar to the case of Fe on GaAs(001). Fe layers grown under these conditions result in a smooth surface morphology, eliminating macroscopic defects as reported previously.[13] In addition, the low growth temperature prevents the formation of Fe_2As[18] or $Fe_3Ga_{2-x}As_x$[10] compounds at the interface, which are considered to be detrimental to the spin-injection efficiency. The thickness of the Fe films was calibrated using *ex situ* x-ray reflectivity (XRR), a technique that can be used to determine the thickness in a wide range from a few to several thousands of angstrom.[29] XRR and high-resolution x-ray diffraction (HRXRD) measurements were done using a PANalytical X'Pert diffractometer system with a Ge(220) hybrid monochromator using Cu $K\alpha_1$ radiation. For the XRR measurement a 0.18° receiving slit was used. Reasonable fits to the experimental XRR curves were obtained by assuming a thin layer of iron oxide of thickness 2.5–2.8 nm, corresponding to approximately 1.5 nm of Fe in agreement with reported values in literature.[30] In Fig. 1 we compare an experimental XRR curve with the simulation of 13-nm-thick Fe and 2.8-nm-thick iron oxide layers on GaAs(113)*A*. From the simulations of XRR profiles we found the interface roughness of the Fe–GaAs interface to be in the range of 0.3–0.8 nm for all thicknesses studied, indicating a rather smooth interface between Fe and GaAs. The initial growth mode and the structure of these films were also studied using *in situ* reflection high-energy electron diffraction (RHEED) with an acceleration voltage of 20 kV. The RHEED pattern from the starting GaAs(113)*A* substrate shows an (8×1) reconstruction with the second-order Laue circle visible, indicating an ordered and smooth surface. The intensity of the specular beam from GaAs decreases drastically after a growth of 1 ML, indicating the formation of disordered islands, and the RHEED pattern was found to be still dominated by the GaAs substrate. After the second monolayer, the RHEED pattern was found to disappear completely and only a diffuse background was seen. The first RHEED pattern from the Fe films was seen at about 4 MLs, suggesting coalescence of islands. For Fe films thicker than 10 MLs, we observe a streaky RHEED pattern along the $[33\bar{2}]$ and $[\bar{1}10]$ azimuths, characteristic of the unreconstructed bcc Fe lattice. The second-order Laue circle was visible for a RHEED pattern along the $[\bar{1}10]$ azimuth. From high-resolution x-ray diffraction (HRXRD) measurements an epitaxial relationship of $Fe(113)[33\bar{2}]\|GaAs(113)[33\bar{2}]$ was confirmed. Magnetic measurements were performed *ex situ*, using a commercial Quantum Design SQUID magnetometer, model MPMS-XL. Samples with thicknesses from 3.5 to 140 MLs were studied in the temperature range of 10–300 K. For SQUID measurements a 20-nm-thick Al capping layer was grown on the Fe layers to prevent oxidation. The growth of the capping layer was also performed at 0 °C to avoid diffusion of Al into Fe.

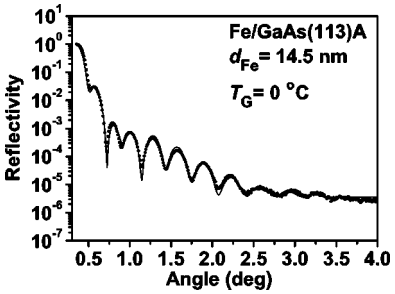

FIG. 1. Measured x-ray reflectivity profile of a 14.5-nm-thick Fe film grown on GaAs(113)*A* (solid dots) and a simulated profile (continuous line).

III. RESULTS

A. Onset of ferromagnetism

A plot of the remanent magnetization M_r versus temperature T for film thicknesses from 4.0 to 30 MLs is shown in Fig. 2. The remanent magnetization M_r is normalized with respect to its value at 10 K, i.e., M_r^0. These measurements were performed while heating the sample from 10 to 300 K. Before the measurement, the samples were magnetized along the $[33\bar{2}]$ direction up to fields large enough to ensure a complete orientation of the magnetic moments. Since all these measurements were made with the magnetic field applied parallel to the easy axis (see Sec. III B), the remanent magnetization is essentially the same as the saturation magnetization. For samples above 10-ML thickness, the RT remanence changes by less than 10% of its value at 10 K, indicating a high Curie temperature of these samples. Thinner samples below 10 MLs show a drastic change in rema-

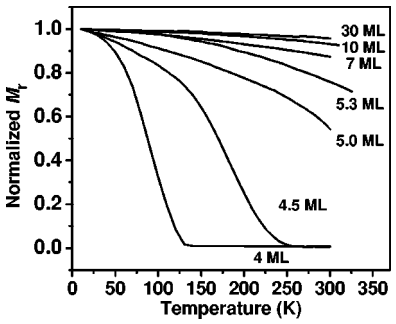

FIG. 2. Temperature dependence of remanent magnetization M_r of Fe/GaAs(113)*A* films having different thicknesses. All curves are normalized with respect to the remanent magnetization at 10 K. Onset of RT ferromagnetic order is between 4.5 and 5.0 MLs.

nence with temperature. The Curie temperature decreases strongly when decreasing the thickness and reaches 120 K for the 4-ML sample. For the 3.5-ML Fe sample we did not observe any ferromagnetism even at 2 K. This implies that the first signature of ferromagnetic order in our films starts between 3.5 and 4.0 MLs. This is approximately the same thickness for which we observe the first RHEED pattern from the Fe layer. The onset of ferromagnetism in these layers can be ascribed to a percolation phenomenon during the coalescence of Fe islands similar to that observed in Fe on GaAs(001).[31,32]

The reader may note that the remanent magnetization versus the temperature curve in Fig. 2 for the 4.0-ML sample having a Curie temperature below RT does not exhibit a behavior typical for an ideal two-dimensional (2D) ferromagnet. The remanent magnetization versus the temperature curve does not drop sharply as expected for an ideal 2D ferromagnet and as observed in the magneto-optical Kerr effect (MOKE) data of Bensch *et al.*[31] for Fe/GaAs(001). In fact, susceptibility versus temperature measurements at an ac frequency of 140 Hz and an ac field of 0.04 Oe shows a peak at 107 K with a full width at half maximum (FWHM) of about 100 K. This large FWHM can be attributed to the averaging measurement method of SQUID magnetometry, which measures the magnetization averaged over the whole sample (several mm^2) in contrast to the MOKE data of Bensch *et al.*,[31] which probes only a small area of the sample. The islanding at the initial stage of growth, in agreement with the RHEED observations, leads to local variations of the Curie temperature within the film and hence to a broadening of the magnetic phase transition. It should be pointed out that a similar behavior was observed in our previous studies of Fe on GaAs(001).[32]

B. In-plane uniaxial magnetic anisotropy in ultrathin films

Figure 3 shows magnetization curves of the 7-ML-thick Fe film ($d_{Fe}=7$ MLs) of Fig. 2 at two different temperatures. These measurements were performed with the magnetic field applied parallel to the two major in-plane perpendicular directions, namely, the $[33\bar{2}]$ and $[\bar{1}10]$ directions. The magnetization curves in Fig. 3 and all other magnetization curves in this article are corrected for the diamagnetic contribution of

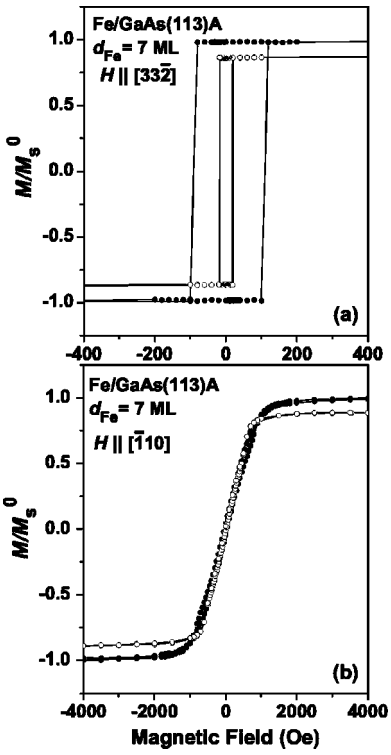

FIG. 3. Magnetization loops of a 7-ML Fe/GaAs(113)*A* film with magnetic field applied in plane along (a) $[33\bar{2}]$ and (b) $[\bar{1}10]$. The open and solid dots are for $T=300$ K (RT) and $T=10$ K, respectively. The magnetization M is normalized to the saturation magnetization at $T=10$ K, M_s^0 after correction for the diamagnetic contribution of the GaAs substrate.

the GaAs substrate. The magnetization M is normalized to the saturation magnetization M_s at $T=10$ K, i.e., M_s^0. As can be seen in Fig. 3, the 7-ML Fe film exhibit a strong UMA with the easy axis along $[33\bar{2}]$. The hysteresis curve along this direction has a pure rectangular shape with a normalized remanence M_r/M_s of about one. This indicates that the Fe layer is essentially single domain in nature or with a preferred domain orientation pointing along the easy axis as suggested for Fe/GaAs(001).[33] An increase in the coercive field at 10 K is observed compared to 300 K. The magnetization curve along the $[\bar{1}10]$ direction does not show any hysteresis, and the coercive field vanishes. The magnetization curve is completely reversible, indicating a hard axis of magnetization. The reversibility of the magnetization curve is suggestive of a rotation process.[8] The in-plane anisotropy field is about 2.5 kOe at 10 K and 1.5 kOe at 300 K. It should be noted that the saturation magnetization for this sample at 300 K decreases to about 10% of its value at 10 K. Moreover, the saturation magnetization for $T\rightarrow 0$ is close to the value of bulk Fe (1740 emu/cm^3), indicating the absence of interfacial Fe–Ga–As compounds.[32] It is noteworthy that the UMA shows a hard axis along the $[\bar{1}10]$ direction similar to the case of Fe on GaAs(001).

C. Four-fold magnetic anisotropy in thick films

We study the evolution of magnetic anisotropy by performing a series of magnetization measurements at RT for Fe film thicknesses varying between 7 MLs and 100 nm. In

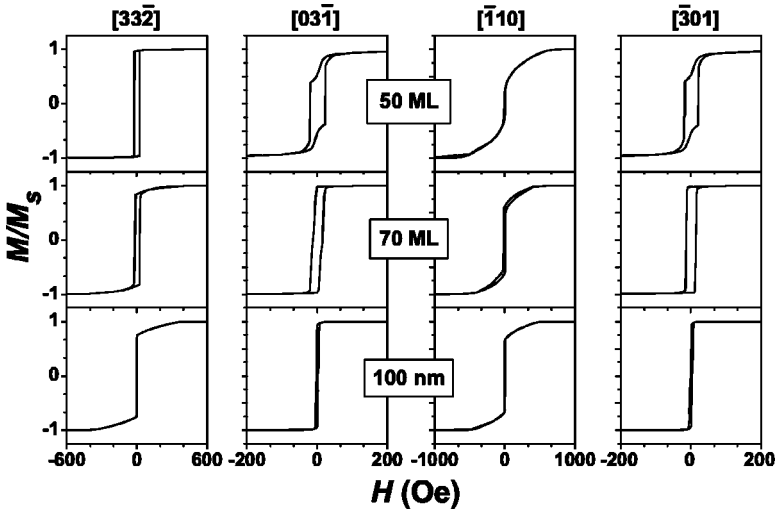

FIG. 4. Magnetization curves of a set of three samples of thicknesses 50 and 70 MLs and 100 nm along the four major in-plane directions at RT, showing the evolution of magnetic anisotropy.

Fig. 4 we show normalized magnetization curves for a set of three selected samples of thicknesses 50 and 70 MLs and 100 nm along the four major in-plane crystallographic axes of the (113) surface, namely, $[33\bar{2}]$, $[\bar{1}10]$, $[03\bar{1}]$, and $[\bar{3}01]$. The $[03\bar{1}]$ and $[\bar{3}01]$ directions lie respectively, at an angle of 42.1° and 137.9° to the $[33\bar{2}]$ direction. The magnetization curve for the 50-ML sample is similar to that of the 7-ML sample of Fig. 3. Hence the 50-ML sample still exhibits a dominant UMA with the easy axis along $[33\bar{2}]$. The magnetization curves of the 70-ML and 100-nm samples, on the other hand, exhibit a dominant four-fold magnetic anisotropy with the easy axes reoriented towards the $[03\bar{1}]$ and $[\bar{3}01]$ directions. The magnetization curves along these directions exhibit a rectangular shape with the normalized remanence of about one. It should be mentioned that the measurement along these two directions has an experimental error of 1°–3°, which arises from a possible misalignment of the sample in the SQUID magnetometer. Note that the in-plane $\langle 03\bar{1}\rangle$ axes can be obtained from the intersection of the (113) plane with the {010} planes. Thus, the observation of the easy axes along these in-plane $\langle 03\bar{1}\rangle$ directions can be considered analogous to the case of Fe on GaAs(001), where the in-plane $\langle 001\rangle$ axes are the easy axes of magnetization. The sample with Fe film thickness of 100 nm shows a normalized remanence of about 0.7 for the magnetic field applied along $[33\bar{2}]$ and $[\bar{1}10]$. Along the $[\bar{1}10]$ direction, a magnetically intermediate direction of bulk Fe, the magnetization curve shows an abrupt transition at a very low field of about 2 Oe, followed by a gradual increase to saturation at approximately 500 Oe. This saturating field of 500 Oe is close to the coercive field calculated from the coherent rotation model for bulk Fe.[8] The saturation magnetization of this 100-nm-thick sample measured along the easy axes is close to the value of bulk Fe, i.e., 1740 emu/cm^3. The RT coercive field along the easy axes is of the order of 7–10 Oe. This reflects the high crystal quality of the Fe films. Hence our results show that the Fe films of and above a 70-ML thickness exhibit a dominant four-fold magnetic anisotropy, whereas Fe films of and below a 50-ML thickness exhibit a dominant UMA. The reorientation of the easy axes occurs in the thickness range from 50- to 70-ML Fe.

To investigate the reorientation phenomenon in more detail, we performed HRXRD measurements on samples having thicknesses varying from 50 MLs to 100 nm. Figures 5(a) and 5(b) show, respectively, the x-ray reciprocal space maps of the diffracted intensity of the two samples of 50- and 70-ML thickness. The measurements were done near the asymmetric (004) reflection of GaAs (in grazing incidence geometry), since the counterpart of the symmetric GaAs(113) reflection is forbidden for Fe. The reciprocal lattice units (rlu) are $\lambda/2d$, where λ is the wavelength of Cu $K\alpha 1$ radiation and d is the lattice plane spacing of the corresponding reflection. The GaAs(004) reflection is located near $Q_x=0.233$ and $Q_y=0.492$. For the 50-ML sample, the layer peak is located at $\Delta Q_x \approx 0$ and $\Delta Q_y=0.0146$, relative to the GaAs substrate where $\Delta Q_{x,y}=Q_{x,y}^{\text{substrate}}-Q_{x,y}^{\text{layer}}$. The parallel mismatch is nearly zero and the layer is completely

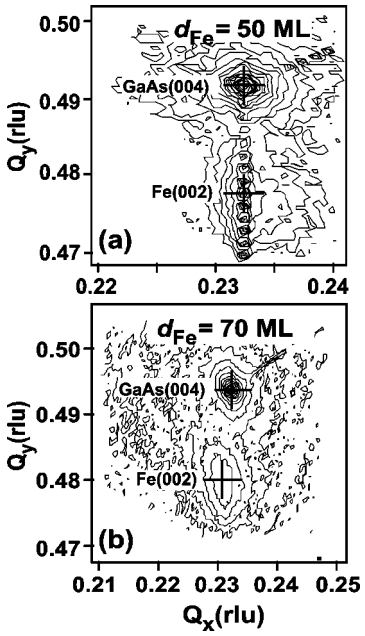

FIG. 5. X-ray reciprocal space map of two samples of thicknesses (a) 50 MLs and (b) 70 MLs for the asymmetric (004) reflection of GaAs, in grazing incidence geometry. The reciprocal lattice units (rlu) are $\lambda/2d$, where λ is the wavelength of Cu $K\alpha 1$ radiation and d is the lattice plane spacing of the corresponding reflection.

strained. In contrast, the layer peak for the 70-ML sample is at $\Delta Q_x = 0.0016$ and $\Delta Q_y = 0.0129$, relative to the GaAs substrate. The parallel mismatch in this case is about 6880 ppm, indicating that the layer is partly relaxed. Pendellösung fringes are visible for the sample of 50-MLs, indicating the good crystal quality of the film. Thus, the relaxation of the layer starts between 50 and 70 MLs, the same thickness range where the reorientation of the easy axes takes place. This indicates that the relaxation of the layer and reorientation of the easy axes of magnetization are apparently correlated. However, we cannot rule out that the reorientation phenomenon and the relaxation of the layer just happen to occur in the same thickness range and are not necessarily related. Thomas *et al.*[19] recently reported that Fe films on GaAs(001) below 60 MLs (exhibiting a dominating UMA) are strained and those above 60 MLs (exhibiting a dominating four-fold anisotropy) are relaxed. Hence, the anisotropic strain relaxation in thicker films had to be taken into account for a quantitative modeling of the magnetic anisotropy as a function of Fe film thickness.

It is important to note that the easy axis of magnetization in thick films ($d_{\mathrm{Fe}} \geqslant 70$ MLs) is found to be along the in-plane $\langle 03\bar{1} \rangle$ axes, which are not the easy axes of magnetization of bulk Fe. In fact, one of the easy axis of bulk Fe, namely the [001] direction, lies out of plane at an angle of 25.24° to the surface normal and towards the $[33\bar{2}]$ direction. However, we found no evidence of a perpendicular easy axis for the magnetic field applied along a set of out-of-plane directions having different inclination angles and measured from the surface normal and towards the in-plane $[\bar{2}33]$ direction. These observations indicate that the demagnetizing energy in this system is very large, and it keeps the magnetization in plane. This is also confirmed by other techniques, including the polar Kerr effect and the extraordinary Hall effect, details of which are discussed elsewhere.[34]

IV. DISCUSSION

The magnetization of Fe/GaAs is often understood by means of a simple rotational mechanism.[15,8,35,36] In order to understand the observed magnetic properties of Fe on GaAs(113)*A*, we use a phenomenological expansion of the free-energy density. The free-energy density of a single domain of magnetization **M** in a magnetic field **H**, with a combination of cubic magnetocrystalline and uniaxial anisotropy can be written as

$$E = K_1[\alpha_1^2\alpha_2^2 + \alpha_1^2\alpha_3^2 + \alpha_2^2\alpha_3^2] + K_2[\alpha_1^2\alpha_2^2\alpha_3^2] + K_u(\mathbf{M}\cdot\mathbf{u}/M)^2 + 2\pi(\mathbf{M}\cdot\mathbf{n})^2 - \mathbf{M}\cdot\mathbf{H}, \quad (1)$$

where K_1 and K_2 are the first two cubic anisotropy constants, K_u is the uniaxial anisotropy constant, and the last two terms refer to the demagnetization energy and Zeeman energy, respectively. Here, α_1, α_2, and α_3 are direction cosines of **M** relative to the cubic crystalline axes. The unit vectors **u** and **n** represent the direction of the uniaxial anisotropy and the surface normal, respectively.

For an in-plane magnetic field, the anisotropy energy density, E_{IPMA} of the (113) surface of Fe can be derived from Eq. (1) by using the direction cosines of the (113) surface symmetry and neglecting the last term, which represents the demagnetization energy. Hence,

$$E_{\mathrm{IPMA}} = (K_1^{\mathrm{eff}}/484)[89 + 16\cos 2\theta_M + 48\cos 4\theta_M] + K_u^{\mathrm{eff}}\sin^2\theta_M - MH\cos\phi. \quad (2)$$

Here θ_M is the angle of magnetization **M** with respect to the unit vector **u**, which is taken along the $[33\bar{2}]$ direction, the observed easy axis of the in-plane UMA. ϕ is the angle of magnetization **M** with respect to the magnetic field **H**. The term involving K_2 is neglected in the above expression, since for bulk Fe and at RT K_2 is smaller than K_1 by two order of magnitudes.[37] In Eq. (2), we have introduced the new constants K_1^{eff} and K_u^{eff} to include the thickness dependence

$$K_1^{\mathrm{eff}} = K_1^{v} + K_1^{\mathrm{int}}/d_{\mathrm{Fe}}, \qquad K_u^{\mathrm{eff}} = K_u^{v} + K_u^{\mathrm{int}}/d_{\mathrm{Fe}}, \quad (3)$$

where K_1^v, K_u^v, K_1^{int}, and K_u^{int} describe the in-plane volume and interface four-fold and uniaxial anisotropy. Here, d_{Fe} is the thickness of the Fe film. $K_{1,u}^{\mathrm{int}}$ is assumed to comprise the contribution of the interface between the magnetic film and the substrate as well as the interface to the Al capping layer, respectively.

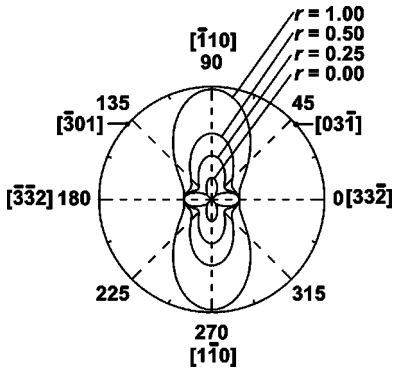

FIG. 6. Polar plot of in-plane anisotropy energy density E_{IPMA} at zero field of the Fe (113) surface according to Eq. (2) for different anisotropy ratio $r = K_u^{\mathrm{eff}}/K_1^{\mathrm{eff}}$. The major in-plane directions are also shown, with zero degree along the $[33\bar{2}]$ direction.

The observed magnetic properties can be qualitatively understood from Eq. (2) above. In Fig. 6 we show a polar plot of Eq. (2) for different anisotropy ratios $r = K_u^{\mathrm{eff}}/K_1^{\mathrm{eff}}$ at zero applied field. The major in-plane directions are also shown, with zero degree along the $[33\bar{2}]$ direction. In the absence of UMA ($r = 0$), there is a minimum in anisotropy energy density at an angle of 47.39° to the $[33\bar{2}]$ direction. When increasing the value of the anisotropy ratio, the minimum in anisotropy energy density moves slowly towards the $[33\bar{2}]$ direction. For $r < 1$, the minimum lies in the neighborhood of the $[03\bar{1}]$ direction which is at an angle of 42.13° to the $[33\bar{2}]$ direction. So, within the experimental uncertainties, the easy axis is detected along the $[03\bar{1}]$ direction. This is the case when the films exhibit a dominant four-fold anisotropy, and this explains the behavior of the samples with $d_{\mathrm{Fe}} \geqslant 70$ MLs (Fig. 4). For large values of the anisotropy

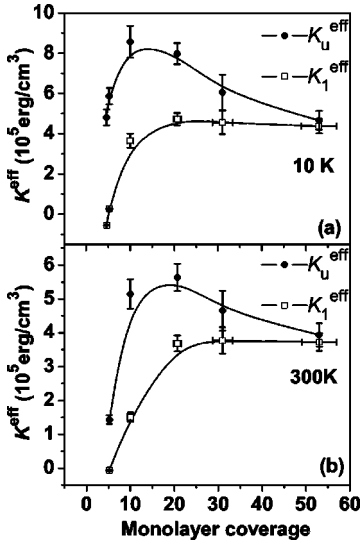

FIG. 7. Plot of K_u^{eff} and K_1^{eff} vs Fe film thickness d_{Fe} at (a) 10 K and (b) 300 K. K_u^{eff} first increases with monolayer coverage up to about 10 MLs and then decreases with thickness, whereas K_1^{eff} increases with thickness and saturates to the bulk value at about 20 MLs.

ratio (i.e., $r \geqslant 1.0$), UMA dominates and the minimum now lies along the $[33\bar{2}]$ direction, which becomes the easy axis. This explains the behavior of the magnetization curves observed for the Fe films of and below 50 MLs in Figs. 4 and 3. Thus, a continuous variation of the anisotropy ratios with thickness can explain the observed magnetic properties.

To get more insight in the magnetic anisotropy constants in dependence of the thickness, we use the hard-axis magnetization curves in the UMA regime to separate the four-fold and the uniaxial magnetic anisotropy. This is done by assuming a reversible rotation along the hard axis $[\bar{1}10]$ similar to that adopted by Brockmann *et al.*[38] for Fe on GaAs(001). An analytical expression for the inverse magnetization loop $H(m)$ can be obtained by minimizing the energy given by Eq. (2) for a magnetic field along $[\bar{1}10]$ ($\phi = \pi/2 - \theta_M$). The resulting expression for $H(m)$ is given by

$$H(m) = K_1^{\text{eff}}(384m^3 - 280m)/121M_s + 2K_u^{\text{eff}}m/M_s, \qquad (4)$$

where $m = M/M_s$ is the normalized component of the magnetization along $[\bar{1}10]$. This is valid in the range of the coherent rotation of the magnetization, i.e., for $-1 < m < 1$. For samples with $d_{\text{Fe}} \leqslant 50$ MLs, the hard-axis magnetization curve along the $[\bar{1}10]$ direction was fitted in the range of $-1 < m < 1$ to yield K_u^{eff} and K_1^{eff}. In Fig. 7 we show plots of K_u^{eff} and K_1^{eff} versus film thickness d_{Fe} at (a) 10 K and (b) 300 K obtained from the fits. For all examined temperatures (10–300 K), K_u^{eff} first increases with the monolayer coverage until about 10 MLs and then decreases with further increase of the monolayer coverage. On the other hand, K_1^{eff} first increases with the monolayer coverage and then saturates to the bulk value after about ~20 MLs. The decrease of K_u^{eff} below 10 MLs is correlated to the structural properties of the Fe films and can be qualitatively understood in terms of the nucleation of Fe islands during the initial stages of growth similar to Fe on GaAs(001).[39,32] To fully understand the thickness dependence of K_u^{eff} after 10 MLs a more extended analysis of the dependence of the effective anisotropy constants on thickness and specially of the separation of volume and interface anisotropy constants is required. Nevertheless, from a comparison of our results with literature[38,39] for Fe/GaAs(001), we believe that this thickness dependence arises from the interfacial nature of the UMA, i.e., K_u^{eff} is a pure interface related term. This is supported by the fact that the fitting of the hard-axis inverse magnetization loop for Fe films below ~5 MLs yields $K_1^{\text{eff}} \simeq 0$; i.e., the magnetization curve in the range of $-1 < m < 1$ is almost linear in this thickness range.

Finally, we address the question on the origin of UMA in the Fe/GaAs(113)*A* system. A particularly interesting possible origin of UMA in Fe on GaAs(113)*A* could be the surface structure of the reconstructed GaAs(113)*A* surface, which exhibit a surface corrugation with step edges parallel to the $[33\bar{2}]$ direction.[20–22] It is known that Fe films grown on stepped surfaces exhibit a uniaxial magnetic anisotropy.[40,41] For Fe on stepped W(001), Chen and Erskine[40] reported a step-induced uniaxial anisotropy with the easy axis perpendicular to the steps, whereas for Fe on stepped Ag(001) Kawakami *et al.*[41] reported an easy axis parallel to the step edges. However, we did not observe any split loop in the magnetization curves like in the cases of Fe on stepped metallic surfaces[40,41] or in other systems, e.g., Co on vicinal Cu(001).[42] Moreover, we observe qualitatively similar magnetic properties in Fe/GaAs(113)*A* compared to Fe/GaAs(001). So we conclude that these reconstruction-induced steps are probably not responsible for the observed UMA. We observe a hard axis along $[\bar{1}10]$, which is also a hard axis for Fe on GaAs(001). The easy axis of UMA in Fe on GaAs(113)*A* found along the $[33\bar{2}]$ direction can be considered as a projection of the [110] axis onto the (113) surface. Hence, the atomic configuration along both of the $[33\bar{2}]$ and [110] directions should be similar. We thus believe that there is a common origin for UMA in the Fe/GaAs(113)*A* and the Fe/GaAs(001) systems. For Fe/GaAs(001), the surface reconstruction of GaAs was shown to be not responsible for the observed UMA.[7,43] Since the uniaxial anisotropy in our samples is found to be originating from the Fe/GaAs interface, we anticipate that the UMA in the Fe/GaAs system is determined by the anisotropy of the bonding between Fe with As and Ga at the Fe–GaAs interface. This is supported by the results of Kneedler *et al.*,[7], where the directional nature of the Fe–As bonding was suggested as an origin of the observed UMA, from a combined scanning tunneling microscopy and Magneto-optic Kerr effect study. A detailed study of the atomic configuration at the Fe–GaAs interface could provide more insight into the microscopic origin of the observed UMA. It should be mentioned that strain anisotropy mediated by magnetoelastic coupling was ruled out as a cause for the observed UMA in thinner Fe films on GaAs(001).[19]

V. CONCLUSIONS

We have investigated the structural and magnetic properties of MBE-grown Fe films on GaAs(113)*A* substrates using RHEED, HRXRD, and SQUID magnetometry. The

SQUID measurements of these Fe films display qualitatively similar magnetic properties compared to Fe on GaAs(001) substrates. The onset of ferromagnetism is observed at a nominal thickness of about 4 MLs, which can be attributed to a percolation phenomenon during the coalescence of Fe islands. The magnetic properties of these films display an intermixing of the four-fold and the uniaxial magnetic anisotropy. For Fe film thicknesses of and below 50 MLs we found a dominating UMA with the easy axis along the in-plane $[33\overline{2}]$ direction. On the other hand, for Fe film thicknesses of and above 70 MLs, we found a dominating four-fold anisotropy with the easy axes along the in-plane $\langle 03\overline{1}\rangle$ directions. The reorientation of the easy axis from the $[33\overline{2}]$ direction to the $\langle 03\overline{1}\rangle$ directions is found to take place between 50 and 70 MLs, the same thickness range where the relaxation of the layer starts. The observed magnetic properties are found to be in good agreement with a simple rotational model of magnetization reversal. By comparing our results with that of Fe on GaAs(001) substrates, a common origin of UMA in Fe/GaAs(113)*A* and Fe/GaAs(001) is suggested. The anisotropy of bonding between Fe with As and Ga at the Fe–GaAs interface is anticipated as a possible origin of the observed UMA.

ACKNOWLEDGMENTS

We would like to thank L. Däweritz, K.-J. Friedland, B. Jenichen, and A. Kawaharazuka for fruitful discussions. Part of this work has been supported by the German BMBF under Contract No. 01BM907.

[1] G. A. Prinz, Science **282**, 1660 (1998).
[2] S. A. Wolf, D. D. Awschalom, R. A. Buhrman, J. M. Daughton, S. von Molnár, M. L. Roukes, A. Y. Chtchelkanova, and D. M. Treger, Science **294**, 1488 (2001).
[3] J. D. Boeck, W. V. Roy, V. Motsnyi, Z. Liu, K. Dessein, and G. Borghs, Thin Solid Films **412**, 3 (2002).
[4] J. R. Waldrop and R. W. Grant, Appl. Phys. Lett. **34**, 630 (1979).
[5] G. A. Prinz and J. J. Krebs, Appl. Phys. Lett. **39**, 397 (1981).
[6] G. A. Prinz, G. T. Rado, and J. J. Krebs, J. Appl. Phys. **53**, 2087 (1982).
[7] E. M. Kneedler, B. T. Jonker, P. M. Thibado, R. J. Wagner, B. V. Shanabrook, and L. J. Whitman, Phys. Rev. B **56**, 8163 (1997).
[8] J. M. Florczak and E. D. Dahlberg, Phys. Rev. B **44**, 9338 (1991).
[9] C. Daboo *et al.*, Phys. Rev. B **51**, 15964 (1995).
[10] A. Filipe, A. Schuhl, and P. Galtier, Appl. Phys. Lett. **70**, 129 (1997).
[11] M. Zölfl, M. Brockmann, M. Köhler, S. Kreuzer, T. Schweinböck, S. Miethaner, F. Bensch, and G. Bayreuther, J. Magn. Magn. Mater. **175**, 16 (1997).
[12] Y. B. Xu, E. T. M. Kernohan, D. J. Freeland, A. Ercole, M. Tselepi, and J. A. C. Bland, Phys. Rev. B **58**, 890 (1998).
[13] H.-P. Schönherr, R. Nötzel, W. Ma, and K. Ploog, J. Appl. Phys. **89**, 169 (2001).
[14] H. J. Zhu, M. Ramsteiner, H. Kostial, M. Wassermeier, H.-P. Schönherr, and K. H. Ploog, Phys. Rev. Lett. **87**, 016601 (2001).
[15] M. Gester, C. Daboo, R. J. Hicken, S. J. Gray, A. Ercole, and J. A. C. Bland, J. Appl. Phys. **80**, 347 (1996).
[16] B. Lépine *et al.*, J. Cryst. Growth **201–202**, 702 (1999).
[17] Y. Chye, V. Huard, M. E. White, and P. M. Petroff, Appl. Phys. Lett. **80**, 449 (2002).
[18] J. J. Krebs, B. T. Jonker, and G. A. Prinz, J. Appl. Phys. **61**, 2596 (1987).
[19] O. Thomas, Q. Shen, P. Schieffer, N. Tournerie, and B. Lépine, Phys. Rev. Lett. **90**, 017205 (2003).
[20] R. Nötzel, N. N. Ledentsov, L. Däweritz, M. Hohenstein, and K. Ploog, Phys. Rev. Lett. **67**, 3812 (1991).
[21] R. Nötzel and K. Ploog, J. Vac. Sci. Technol. A **10**, 617 (1992).
[22] M. Wassermeier, J. Sudijono, M. D. Johnson, K. T. Leung, B. G. Orr, L. Däweritz, and K. Ploog, Phys. Rev. B **51**, 14721 (1995).
[23] R. Nötzel, N. N. Ledentsov, L. Däweritz, K. Ploog, and M. Hohenstein, Phys. Rev. B **45**, 3507 (1992).
[24] R. Nötzel, Microelectron. J. **28**, 875 (1997).
[25] R. Nötzel, J. Menniger, M. Ramsteiner, A. Trampert, H. P. Schönherr, L. Döweritz, and K. H. Ploog, J. Cryst. Growth **175**, 1114 (1997).
[26] R. Nötzel *et al.*, Appl. Phys. Lett. **72**, 2002 (1998).
[27] R. Nötzel, Z. C. Niu, M. Ramsteiner, H.-P. Schönherr, A. Trampert, L. Däweritz, and K. H. Ploog, Nature (London) **392**, 56 (1998).
[28] R. Nötzel, Q. Gong, M. Ramsteiner, U. Jahn, K.-J. Friedland, and K. H. Ploog, Microelectron. J. **33**, 573 (2002).
[29] A. Richter, R. Guico, and J. Wang, Rev. Sci. Instrum. **72**, 3004 (2001).
[30] A. J. Melmed and J. J. Carroll, J. Vac. Sci. Technol. **10**, 164 (1973).
[31] F. Bensch, G. Garreau, R. Moosbühler, and G. Bayreuther, J. Appl. Phys. **89**, 7133 (2001).
[32] J. Herfort, W. Braun, A. Trampert, H. P. Schönherr, and K. H. Ploog, Appl. Surf. Sci. **237**, 181 (2004).
[33] C. M. Boubeta, A. Cebollada, J. F. Calleja, C. Contreras, F. Peiró, and A. Cornet, J. Appl. Phys. **93**, 2126 (2003).
[34] K. J. Friedland, P. K. Muduli, J. Herfort, H.-P. Schönherr, and K. H. Ploog (unpublished).
[35] E. Gu, J. A. C. Bland, C. Daboo, M. Gester, L. M. Brown, R. Ploessl, and J. N. Chapman, Phys. Rev. B **51**, 3596 (1995).
[36] K. T. Riggs, E. D. Dahlberg, and G. A. Prinz, Phys. Rev. B **41**, 7088 (1990).
[37] B. D. Cullity, in *Introduction to Magnetic Materials*, 1st ed. (Addison-Wesley, Reading, MA, 1972), p. 234.
[38] M. Brockmann, M. Zölfl, S. Miethaner, and G. Bayreuther, J. Magn. Magn. Mater. **198–199**, 384 (1999).
[39] F. Bensch, R. Moosbühler, and G. Bayreuther, J. Appl. Phys. **91**, 8754 (2002).
[40] J. Chen and J. L. Erskine, Phys. Rev. Lett. **68**, 1212 (1992).
[41] R. K. Kawakami, E. J. Escorcia-Aparicio, and Z. Q. Qiu, Phys. Rev. Lett. **77**, 2570 (1996).
[42] R. K. Kawakami, M. O. Bowen, H. J. Choi, E. J. Escorcia-Aparicio, and Z. Q. Qiu, Phys. Rev. B **58**, R5924 (1998).
[43] R. Moosbühler, F. Bensch, M. Dumm, and G. Bayreuther, J. Appl. Phys. **91**, 8757 (2002).